the calls. We played the 1-min playback sequence a single time and continued to note number of animals and distance to the nearest animal for an additional 2 min or more. Before playbacks the average number of seals at the surface was 13.6 (standard deviation, std, 7.9), and the average distance of the nearest seal to the playback source was 60.2 m (std 21.3 m). Trials where fewer than five seals were present before the playback were excluded from the analysis. The strength of the response was expressed as the percentage change in the average number of seals and average distance to the nearest seal from the 2 min before to the 2 min after the calls were played. Playback experiments were conducted off northern Vancouver Island in Johnstone and Queen Charlotte Straits and off southern Vancouver Island in Haro and Georgia straits.

Experiment 1

Test and control playbacks were conducted once each at the same haulout in random order at the same tidal height on consecutive days. Both types of playback sequences were based on identical sections of background noise from a digitized recording of transient killer whales digitally spliced into a 1-min sequence. Sections containing whistles, echolocation clicks or pulsed calls were not used for this purpose. To avoid startle responses caused by the sudden onset of unfamiliar background noise, the volume was slowly faded in over the first 30 s of the sequence and faded out during the last 10 s. For test sequences, five killer whale calls from the same recording, belonging to at least three different call types, were spliced into the sequence between the fades. For control sequences an additional five sections of background noise were spliced in instead of the calls. The volume of each sequence pair was adjusted so that the loudest call in the test sequence had a source level of 148 dB (reference pressure 1 μPa at 1 m). We generated and used four such pairs of sequences from recordings of different transient groups and played each at two different haulouts. In order to avoid pseudoreplication[24], we averaged responses obtained at haulouts where the same pair of playback sequences was played, so that the number of playback sequences, not trials, determined degrees of freedom. We used a paired t-test to test for significant differences between responses to test and control.

Experiment 2

For this experiment, we generated three types of playback sequence using the methodology explained above. Sequences for playbacks of familiar fish-eater calls contained five calls from BC resident killer whales. We used calls of northern residents for playbacks off northern Vancouver Island, and those of southern residents off southern Vancouver Island. For playbacks of unfamiliar killer whale calls we generated sequences from recordings of Alaskan residents made in Prince William Sound, Alaska. Sequences of transient calls were those used as test sequences in experiment 1. Except for the familiar fish-eating killer whales, we generated four sequences for each playback type from recordings of different social groups. For familiar fish-eating killer whales, we generated a total of seven playback sequences (three of northern residents and four of southern residents). Ten trials were conducted for each playback type and again, to avoid pseudoreplication, all responses obtained with the same playback sequence were averaged. We used a one-way ANOVA to test for statistical differences between the playback types and used Tukey's honestly significant difference test[25] to determine which playback types differed.

1. Tuttle, M. D. & Ryan, M. J. Bat predation and the evolution of frog vocalizations in the neotropics. *Science* **214**, 677–678 (1981).
2. Gliwicz, M. Z. Predation and the evolution of vertical migration in zooplankton. *Nature* **320**, 746–748 (1986).
3. Rattenborg, N. C., Lima, S. L. & Amlaner, C. J. Half-awake to the risk of predation. *Nature* **397**, 397–398 (1999).
4. Lorenz, K. Vergleichende Verhaltensforschung. *Verhand. Deutsch. zool. Gesselschaft* **1939**, 69–102 (1939).
5. Tinbergen, N. Social releasers and the experimental method required for their study. *Wilson Bull.* **60**, 6–51 (1948).
6. Ford, J. K. B. *et al.* Dietary specialization in two sympatric populations of killer whales (*Orcinus orca*) in coastal British Columbia and adjacent waters. *Can. J. Zool.* **76**, 1456–1471 (1998).
7. Saulitis, E., Matkin, C., Barrett-Lennard, L., Heise, K. & Ellis, G. Foraging strategies of sympatric killer whale (*Orcinus orca*) populations in Prince William Sound. *Mar. Mamm. Sci.* **16**, 94–109 (2000).
8. Bigg, M. A., Olesiuk, P. F., Ellis, G. M., Ford, J. K. B. & Balcomb, K. C. Social organization and genealogy of resident killer whales (*Orcinus orca*) in the coastal waters of British Columbia and Washington State. *Rep. Int. Whal. Commission (spec. issue)* **12**, 383–405 (1990).
9. Hoelzel, R. A. & Dover, G. A. Genetic differentiation between sympatric killer whale populations. *Heredity* **66**, 191–196 (1991).
10. Hoelzel, A. R., Dahlheim, M. & Stern, S. J. Low genetic variation among killer whales (*Orcinus orca*) in the eastern North Pacific and genetic differentiation between foraging specialists. *J. Hered.* **89**, 121–128 (1998).
11. Barrett-Lennard, L. G. *Population Structure and Mating Patterns of Killer Whale Populations in the Northeastern Pacific, as Revealed by DNA Analysis.* PhD thesis, Univ. British Columbia (2000).
12. Ford, J. K. B. Acoustic behaviour of resident killer whales (*Orcinus orca*) off Vancouver Island, British Columbia. *Can. J. Zool.* **67**, 727–745 (1989).
13. Barrett-Lennard, L. G., Ford, J. K. B. & Heise, K. A. The mixed blessing of echolocation: Differences in sonar use by fish-eating and mammal-eating killer whales. *Anim. Behav.* **51**, 553–565 (1996).
14. Ford, J. K. B. Vocal traditions among resident killer whales (*Orcinus orca*) in coastal waters of British Columbia, Canada. *Can. J. Zool.* **69**, 1454–1483 (1991).
15. Yurk, H., Barrett-Lennard, L., Ford, J. K. B. & Matkin, C. O. Cultural transmission within maternal lineages in resident killer whales in Southern Alaska. *Anim. Behav.* **63**, 1103–1119 (2002).
16. Deecke, V. B., Ford, J. K. B. & Spong, P. Dialect change in resident killer whales (*Orcinus orca*): Implications for vocal learning and cultural transmission. *Anim. Behav.* **60**, 619–638 (2000).
17. Møhl, B. Auditory sensitivity of the common seal in air and water. *J. Aud. Res.* **8**, 27–38 (1968).
18. Miller, P. J. O. *Maintaining Contact: Design and Use of Acoustic Signals in Killer Whales*, Orcinus orca. PhD thesis, Joint Program in Oceanography/Applied Ocean Science and Engineering, Woods Hole Oceanographic Institution and Massachusetts Institute of Technology (2000).
19. Nichol, L. M. & Shackleton, D. M. Seasonal movements and foraging behaviour of northern resident killer whales (*Orcinus orca*) in relation to the inshore distribution of salmon (*Oncorhynchus* ssp.) in British Columbia. *Can. J. Zool.* **74**, 983–991 (1996).
20. Schleidt, W. M. Über die Auslösung der Flucht vor Raubvögeln bei Truthühnern. *Naturwissenschaften* **5**, 141–142 (1961).
21. Wiley, R. H. in *Behavioral Mechanisms in Evolutionary Ecology* (ed. Real, L. A.) 157–189 (Univ. Chicago Press, Chicago, IL, 1994).
22. Bradbury, J. W. & Vehrencamp, S. L. *Principles of Animal Communication* (Sinauer, Sunderland, MA, 1998).
23. Curio, E. Proximate and developmental aspects of antipredator behavior. *Adv. Study Behav.* **22**, 135–238 (1993).
24. Kroodsma, D. E. Suggested experimental design for song playbacks. *Anim. Behav.* **37**, 600–609 (1989).
25. Zar, J. C. *Biostatistical Analysis* (Prentice Hall, Upper Saddle River, NJ, 1996).

Graded persistent activity in entorhinal cortex neurons

Alexei V. Egorov*, Bassam N. Hamam*, Erik Fransén†, Michael E. Hasselmo‡ & Angel A. Alonso*

* *Department of Neurology and Neurosurgery, Montreal Neurological Institute and McGill University, Montreal, Quebec H3A 2B4, Canada*
† *Department of Numerical Analysis and Computer Science, Royal Institute of Technology, S-100 44 Stockholm, Sweden*
‡ *Department of Psychology, Program in Neuroscience and Center for Memory and Brain, Boston University, Boston, Massachusetts 02215, USA*

Working memory represents the ability of the brain to hold externally or internally driven information for relatively short periods of time[1,2]. Persistent neuronal activity is the elementary process underlying working memory but its cellular basis remains unknown. The most widely accepted hypothesis is that persistent activity is based on synaptic reverberations in recurrent circuits. The entorhinal cortex in the parahippocampal region is crucially involved in the acquisition, consolidation and retrieval of long-term memory traces for which working memory operations are essential[2]. Here we show that individual neurons from layer V of the entorhinal cortex—which link the hippocampus to extensive cortical regions[3]—respond to consecutive stimuli with graded changes in firing frequency that remain stable after each stimulus presentation. In addition, the sustained levels of firing frequency can be either increased or decreased in an input-specific manner. This firing behaviour displays robustness to distractors; it is linked to cholinergic muscarinic receptor activation, and relies on activity-dependent changes of a Ca^{2+}-sensitive cationic current. Such an intrinsic neuronal ability to generate graded persistent activity constitutes an elementary mechanism for working memory.

The entorhinal cortex (EC) is a crucial component of the medial temporal-lobe memory system[4,5]. EC neurons have been shown to display persistent activity during the delay phase of delayed match or non-match to sample memory trials[6,7] and the hippo-

campal–parahippocampal region is important in paired-associate learning[6,8–10].

Layer V neurons of the EC receive convergent sensory input from cortex[11,12], are the target of hippocampal output[13], and give rise to a massive backward projection to the cortex[3]. EC layer V is also densely innervated by cholinergic fibres from the basal forebrain[14]. Cholinergic muscarinic influences have been shown to be vital to memory processes[15] and muscarinic actions have profound effects on the intrinsic firing pattern of neurons[16]; we therefore investigated by means of intracellular recordings in a rat EC slice preparation whether muscarinic actions could induce mnemonic activity in EC layer V cells.
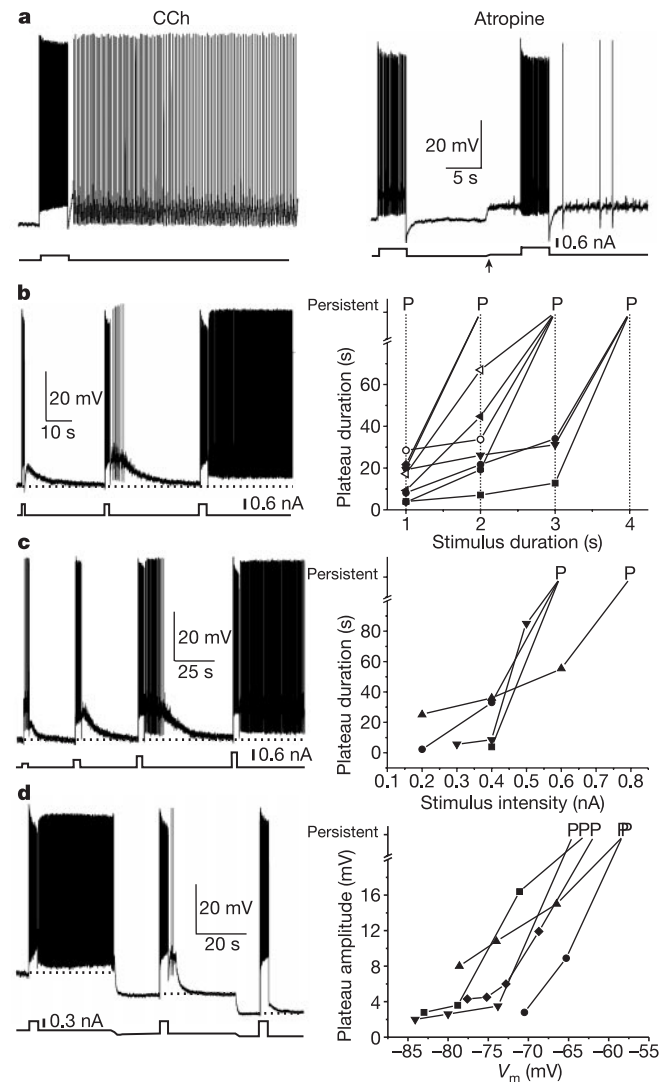
Figure 1 Muscarinic-dependent persistent activity. **a**, CCh-induced persistent firing (5 μM; left) and block by atropine (1 μM; right). The arrow below the right current trace signals an imposed direct current (d.c.) shift. **b**, **c**, Left panels show responses to current steps of increasing duration (**b**) and amplitude (**c**) in a representative neuron (CCh, 10 μM). Right panels show plots of plateau duration versus stimulus duration (**b**) and intensity (**c**) (different symbols correspond to different neurons; in **b**, closed and open symbols correspond to the same neuron studied at a lower and higher stimulus intensity, respectively). **d**, Left panel shows voltage dependence of persistent firing. Right panel shows plot of plateau-potential amplitude as a function of membrane potential (V_m). In all plots, the letter P indicates the transition to persistent firing. In this and Figs 2 and 4, recordings were performed during neurotransmission block as detailed in the Methods. Initial V_m in **a**, **b**, **c** and **d** is −59 mV, −64 mV, −65 mV and −62 mV.

In this study we found that in electrophysiologically identified EC layer V principal cells[17], bath application of the cholinergic agent carbachol (CCh) (5 μM, $n = 38$; 10 μM, $n = 49$) blocked the slow afterhyperpolarization that follows a train of action potentials and, in most cases (84% and 98% in 5 μM and 10 μM CCh, respectively), triggered the development of a slow depolarizing afterpotential that could give rise to a plateau potential accompanied by spiking (Fig. 1). This plateau potential relied on the activation of muscarinic receptors since its induction was blocked by 1 μM atropine ($n = 3$; Fig. 1a) or 1 μM pirenzepine ($n = 4$) and it could also be induced by bath superfusion with muscarine (5, 10 μM, $n = 11$). The muscarinic-dependent plateau potential and all of its properties were not caused by local circuit reverberation mechanisms, because we commonly studied them during glutamatergic and GABA-mediated neurotransmission block (as specified in Methods). Nevertheless, the plateau activity could be induced equally well with synaptic stimulation during intact neurotransmission ($n = 7$; see below).

Muscarinic-dependent plateau potentials have been described in several cortical neuronal populations[18–20] including principal cells from EC layer II[21], where they could provide a cellular mechanism for the delayed activity observed during working memory tasks[22]. However, the plateau potentials observed in EC layer II neurons always self-terminate[21]. In contrast, we found that when EC layer V cells were activated from a resting level of about 10 mV or less from spike threshold, increases in the stimulus duration (Fig. 1b) or intensity (Fig. 1c) always led to an increase in the duration of the plateau potential (Fig. 1b and c, right-hand plots), which could then give rise to a stable state of sustained spiking for an apparently indefinite period of time (Fig. 1b–d) (tested up to 13 min, although we typically interrupted it after about 40–60 s). This therefore represents the muscarinic- and activity-dependent induction of a self-sustained state of stable firing. We tested responses to current-step durations that ranged from about 0.3 to 8 s and of intensities that commanded spike trains of 15–40 Hz, which is in the beta/low-gamma range of frequencies characteristic of limbic cortices during active states[23]. While there was some cell-to-cell variability with respect to the stimulus parameters that elicited persistent firing (Fig. 1b–d), we found that the phenomenon was very robust as it could be elicited in the vast majority of neurons that expressed plateau potentials (see below) and, in every single cell that expressed persistent firing, it could be re-elicited for as long as the recording was maintained. The plateau potential that sustained persistent firing displayed very pronounced voltage dependence. When stimuli of equivalent strength were presented from increasingly negative resting levels, plateau-potential amplitude decreased sharply with membrane hyperpolarization, and persistent firing could never be elicited by stimulation from voltage levels below about −70 mV (Fig. 1d). The ability of neurons to express persistent firing increased with CCh concentration. At a CCh concentration of 10 μM, a 4-s-long spike train at 15–40 Hz that was evoked from a resting level of about 10 mV or less from spike threshold almost invariably elicited persistent activity (95% of neuron tested; $n = 39$); we therefore chose 4 s as our standard stimulation duration for most of our analysis. However, stimulus durations in the range of 0.3 to 1 s could also be effective in triggering persistent firing in many neurons (8 out of 11 tested; Supplementary Fig. A). At a CCh concentration of 5 μM, a stimulus of about 4 s in duration elicited persistent activity in 86% of neurons tested ($n = 28$).

Persistent activity for working memory can directly encode dimensions of input or output signals if it can maintain stable analogue values of activity[24]. We therefore tested whether repetitive application of a given activating stimulus could give rise to a series of graded increases of stable discharge rates. Thus, might muscarinic actions implement in EC layer V neurons the ability to behave as 'neural integrators'? Indeed, as in Fig. 2a (see also Supplementary Information), repetitive application of an input that would give rise

to a state of sustained firing always led to well-defined increases of stable discharge rates in all neurons tested ($n = 13$ in $10\,\mu M$ CCh and $n = 8$ in $5\,\mu M$ CCh). These increases consisted of three to seven levels up to a ceiling (Fig. 2a) where no further enhancement in firing rate was observed. The average maximum persistent firing frequency induced in this manner was $9.8 \pm 4.6\,Hz$ ($n = 9$) in $10\,\mu M$ CCh and $8.5 \pm 2.9\,Hz$ ($n = 7$) in $5\,\mu M$ CCh.

Once persistent firing was initiated we noticed that it could only be turned off by prolonged membrane hyperpolarizations (Figs 2c and 3a). The larger the amplitude of the hyperpolarization, the shorter the time required to turn off the persistent active state, but durations of at least 5–10 s for hyperpolarizations to about 80 mV were required to fully stop persistent firing. Graded increases in firing frequency can be effected by repetitive activating stimuli, so

we examined whether repetitive application of hyperpolarizing current pulse steps would have the opposite effect; that is, lead to graded stable decreases in firing rate ($n = 8$). Indeed, as in the case illustrated in Fig. 2c, discrete decreases in firing rate could always be obtained by repetitive step hyperpolarizations of duration equal to, or longer than, those used to induce persistent firing.

Given the unique phenomenon of intrinsic persistent firing elicited by current-step-driven spike trains, we tested whether local synaptic activation could also lead to a state of persistent firing. As illustrated in Fig. 3a, during intact neurotransmission, plateau potentials that sustained stable firing could either be induced by transiently activating the cells synaptically at about 10–20 Hz or by step depolarizations in all neurons examined ($n = 7$). In addition, graded increases in persistent firing frequency
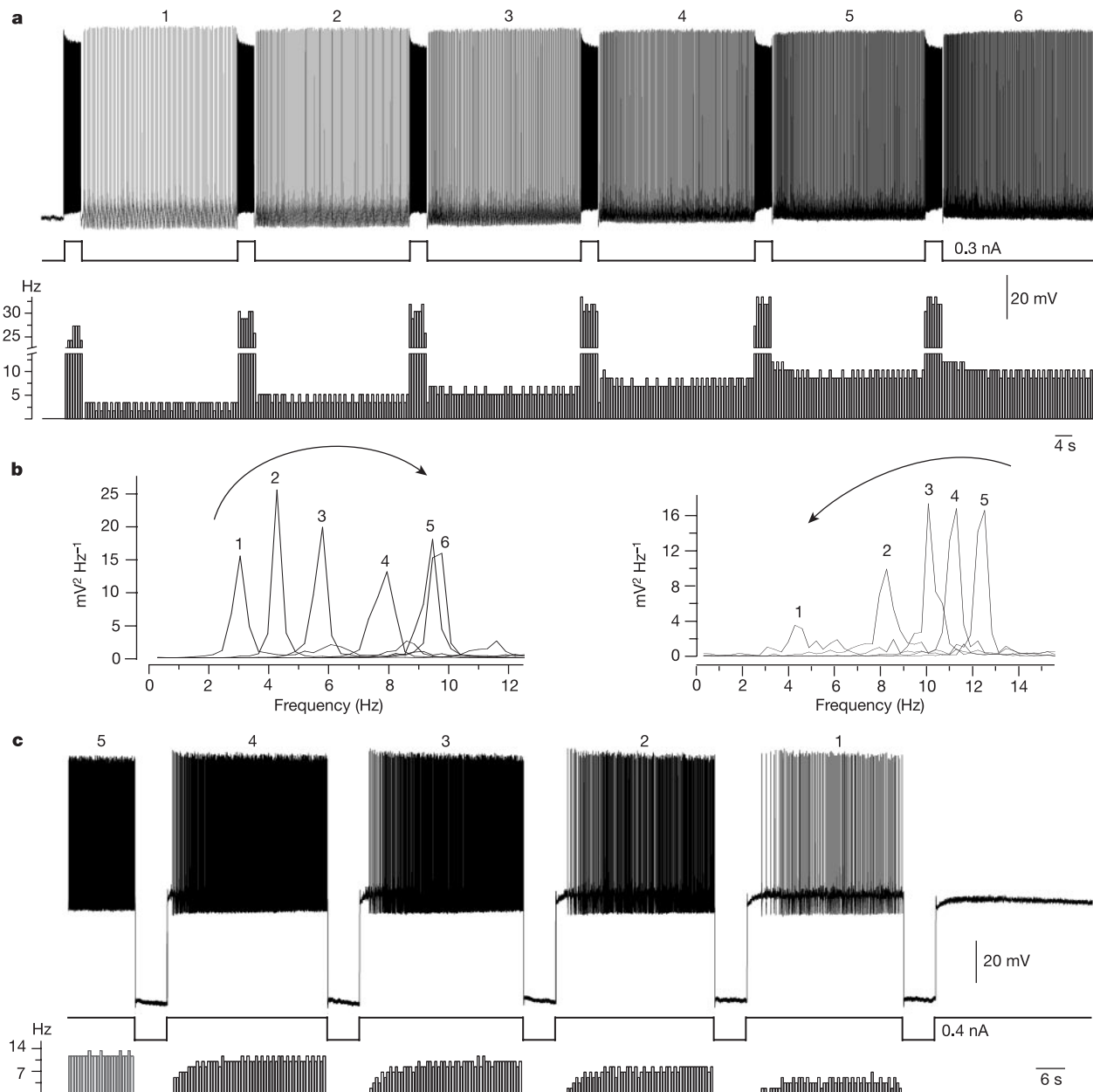
Figure 2 Graded persistent activity. **a**, Repetitive stimulation with a 4-s depolarizing step gives rise to five distinct increases (traces 1 to 6) of stable discharge rate (CCh, $10\,\mu M$). **b**, Fourier analysis plots for the corresponding numbered segments in **a** (left) and **c** (right). **c**, Repetitive application of 6-s hyperpolarizing steps gives rise to discrete decreases of stable discharge rate and to the eventual cessation of firing (CCh, $5\,\mu M$). The lower diagrams in **a** and **c** correspond to the peristimulus histograms (bin width of 580 ms). Initial V_m in **a** is $-64\,mV$. Final V_m in **b** is $-55\,mV$.

could also be produced by repetitive activation with a synaptic train in all cases tested ($n = 4$) (Fig. 3b). In order to examine whether graded decreases in stable frequency could also be produced by synaptic inhibition, we tested neurons during partial glutamatergic neurotransmission block with 1 mM kynurenic acid. In most cases ($n = 12$ out of 14), we observed that synaptic inhibition was also capable of producing stable decreases in firing frequency (Fig. 3c).

The above data indicate that muscarinic modulation of EC layer V neurons implements in these neurons the internal ability to generate truly persistent activity that can maintain multiple levels of stable firing rate. Another important property of mnemonic persistent activity is that it should be resistant to distracting inputs. We also found that states of stable firing frequency were not affected by relatively brief excitatory–inhibitory stimuli (Supplementary

Fig. B). Typically, current-step-driven spike trains of insufficient strength to elicit persistent firing were also unable to produce graded changes in firing frequency. Similarly, step membrane hyperpolarizations of about 20 mV and shorter than 2 s were always ineffective in causing graded decreases in firing frequency.

Finally, we pharmacologically explored the ionic mechanism underlying the generation of intrinsic persistent activity in layer V cells. The activity-dependent characteristics of the plateau potentials in these neurons clearly suggest that Ca^{2+} influx associated with spiking is an important element. We found that abolishing Ca^{2+} influx by removal of extracellular Ca^{2+} completely and reversibly blocked the muscarinic induced plateau potentials ($n = 4$; Fig. 4a). Similarly, intracellular injection of the Ca^{2+} chelator EGTA also abolished the plateau activity ($n = 3$), thus
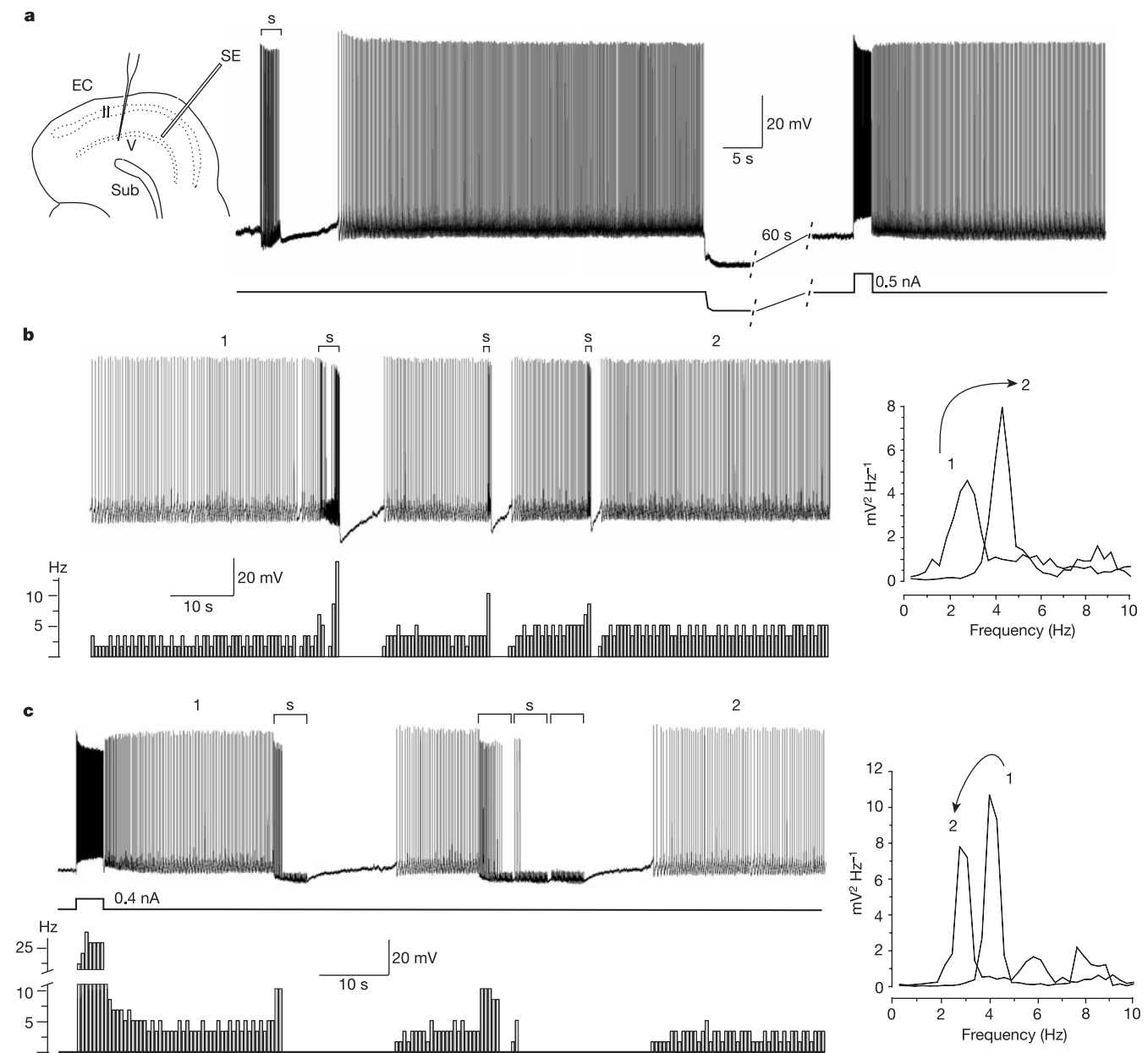
Figure 3 Synaptic induction of persistent activity. **a**, A synaptic train (10 Hz, 2.4 s) induces persistent firing which is then stopped by hyperpolarization and re-initiated by current step depolarization (CCh, 10 μM). Left, schematic representation of the position of recording and stimulating (SE) electrodes. **b**, Stable increase in persistent firing frequency by synaptic excitation (20 Hz; CCh, 10 μM). **c**, Stable decrease in persistent firing frequency by synaptic inhibition (10 Hz; CCh, 5 μM; kynurenic acid, 1 mM). Right plots: Fourier analysis for the corresponding labelled segments. Segments labelled as 's' correspond to periods of synaptic stimulation. Initial V_m in **a** and **c** is −62.5 mV and − 62 mV.
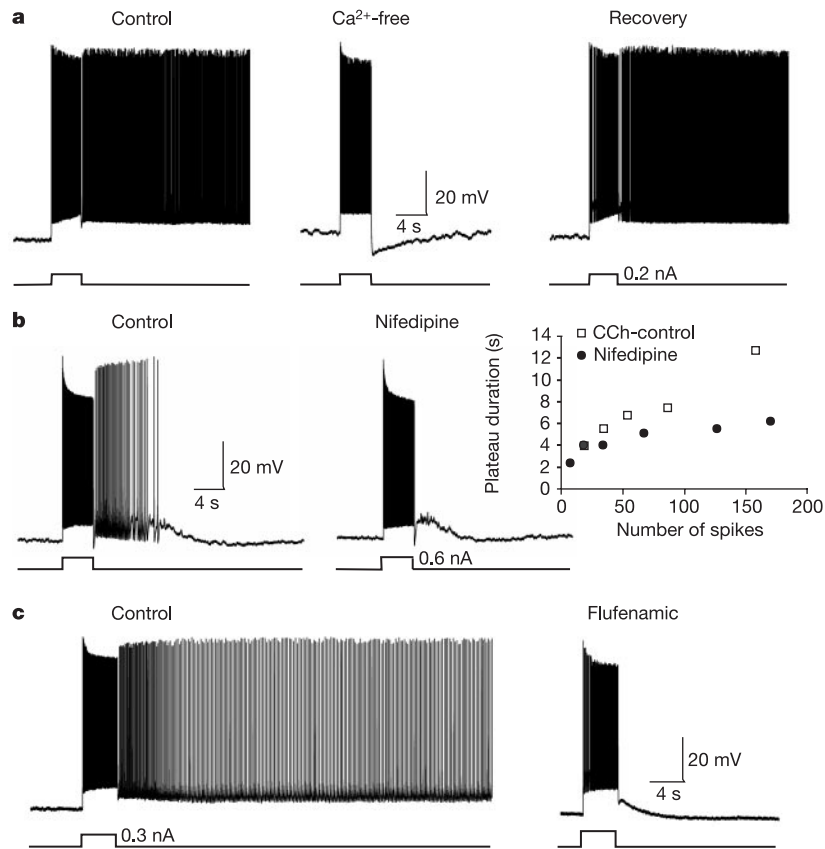
Figure 4 Persistent activity requires activity-dependent Ca^{2+} influx and a non-specific cation current. **a**, Persistent response (left) abolished by removal of extracellular Ca^{2+} (middle) with recovery (right) after Ca^{2+} reintroduction (CCh, 5 μM). **b**, Persistent activity and plateau potentials were partially blocked by the L-type Ca^{2+} channel blocker nifedipine (50 μM; CCh, 5 μM). The right diagram illustrates the decrease in the slope of the plot of plateau duration versus stimulus intensity (number of spikes in the triggering train) induced by nifedipine. **c**, Complete block of persistent activity by flufenamic acid (10 μM; CCh, 10 μM). Initial V_m in **a**, **b** and **c** is −65 mV, −60 mV and −66 mV.

indicating its dependence on intracellular Ca^{2+} rises. Because spiking is expected to lead to Ca^{2+} influx through, at least, high-voltage activated Ca^{2+} channels, we then tested the effect of the L-type Ca^{2+}-channel blocker nifedipine (50 μM) on the plateau activity. In all cases ($n = 6$), nifedipine partially blocked the plateau potentials and curtailed the ability of the cells to generate persistent activity (Fig. 4b). Finally, the possibility that the Ca^{2+}-dependent plateau potentials were mediated by a Ca^{2+}-activated non-specific cation current was tested: we assessed the effects of the Ca^{2+}-activated non-specific current-blocking agent flufenamic acid (10 μM) (ref. 25), which always ($n = 4$) blocked the cells' ability to generate plateau potentials (Fig. 4c). The above findings point to spike-induced Ca^{2+} influx triggering a slow potential mediated by a cationic current as a basic mechanism for the generation of persistent activity.

Computational modelling studies have shown that recurrent reverberatory circuits can give rise to persistent activity, provided the synaptic feedback has a slow kinetics[24,26,27]. However, our data *in situ* demonstrate that a non-synaptic spike- and Ca^{2+}-induced potential is, in fact, sufficient for the generation of prolonged persistent activity which can be graded in a stimulus-specific manner. EC layer V neurons lie at the core of the hippocampal–neocortical memory system, which implements the acquisition, storage and retrieval of memories for facts and events in a temporally organized and graded manner. The implementation of this type of single-cell mnemonic mechanism, which allows cells to 'hold on' to information for relatively prolonged periods of time and enables the system to perform associational computations,

might be fundamental for the memory operations in the temporal lobe.

Sensory information converges into the EC following a cascade of cortico-cortical projections[28]. We found that while short stimuli (about 500 ms) could be effective in triggering graded persistent firing, longer stimuli were more effective. This is not surprising since the input to EC layer V neurons may already consist of prolonged discharges from previous stages in the associational hierarchy[1,2,7]. It has been suggested that while working memory operations in prefrontal cortex may be important for monitoring familiar stimuli, the medial temporal lobe may be more important for matching and active maintenance of new information during memory delays[10]. The intrinsic persistent activity displayed by the EC layer V cells represents an ideal mechanism for sustaining information about a new stimulus for memory encoding and/or consolidation purposes. In this respect, EC layer V gives rise to feedback cortical projections, and lesions of the EC have been shown to prevent inferotemporal neurons from representing associations between visual stimuli[9].

Thus, we have shown that muscarinic cholinergic actions allow EC layer V neurons to behave through a non-synaptic mechanism as analogue memory devices. In contrast to bistable neurons[29], they can store multiple bits of information in the form of their activity along a graded dimension determined by stimulus input. We propose that this intrinsic cellular behaviour constitutes an elementary form of mnemonic process on which associative network mechanisms could build to hold externally or internally driven sensory representations. □

letters to nature

Methods

Preparation of brain slices

Brain slices were obtained from male Long Evans rats (150–250 g, Charles River, Canada) using standard procedures[21]. Briefly, animals were deeply anaesthetized with halothane and decapitated; the brain was then rapidly removed, and placed in a cold (4–6 °C) oxygenated Ringer solution containing (in mM): 124 NaCl, 3 KCl, 1.6 CaCl$_2$, 1.8 MgSO$_4$, 26 NaHCO$_3$, 1.25 NaH$_2$PO$_4$ and 10 glucose (pH maintained at 7.4 by saturation with 95%O$_2$/5%CO$_2$). A block of tissue containing the retrohippocampal region was then dissected out and 400-μm-thick horizontal slices of the entorhinal cortex (EC) were obtained using a vibratome (Pelco). Slices were then incubated in an interface holding chamber at room temperature for >1 h before use. Individual slices were transferred to the interface recording chamber (Fine Scientific tools) one by one, superfused with Ringer solution at a rate of 1–2 ml min^{-1}, and maintained at 34 °C ± 1 °C. Layer V of the entorhinal cortex was identified with a dissecting microscope by transillumination.

Recording procedures, drugs and analysis

Intracellular recordings were obtained using sharp microelectrodes pulled on a Brown-Flaming puller P-87 (Sutter Instruments) from 1.5 mm borosilicate glass (Sutter Instruments). Electrodes were backfilled with 2 M K$^+$-acetate (tip resistance of 90–120 MΩ). Signals were amplified using an Axoclamp 2A amplifier, digitized at 5 KHz (Digidata 1200, Axon Inst.) and stored on a Pentium computer, and visualized using AxoScope software (Axon Inst.). Most recordings were performed during glutamatergic and GABA-mediated neurotransmission block with drug cocktails consisting of either a mixture of kynurenic acid (1–10 mM) and picrotoxin (100 μM) ($n = 81$), or a mixture of DL-2-amino-5-phosphonovaleric acid (50 μM), 6-cyano-7-nitroquinoxaline-2,3-dione (10 μM) and picrotoxin (100 μM) ($n = 7$). Synaptic transmission was blocked in most experiments to ensure that the phenomena studied were independent of synaptic transmission. Carbachol, muscarine, atropine and pirenzepine were bath-applied at the desired concentrations from stock solutions (10 mM for CCh and 10 mM for muscarine) in distilled water. Because the muscarinic phenomena studied did not desensitize, in many cases the neurons were directly impaled in the presence of CCh. The resting membrane potential of the neurons was −70.5 ± 3 mV ($n = 17$) in control Ringer, and −63.7 ± 5 mV ($n = 36$) and −62.8 ± 5.5 mV ($n = 47$) in the presence of 5 and 10 μM CCh, respectively. We chose these levels of CCh because in a previous study using the same EC slice preparation we found that higher CCh concentrations led to the production of epileptiform events[30]. Flufenamic acid and nifedipine were applied from stock solutions made in DMSO so that the final concentration of DMSO in Ringer was ≤0.1%. Control experiments revealed no measurable effects of DMSO on cellular properties or cholinergic modulatory actions ($n = 4$). The Ca^{2+}-free solution contained 6 mM Mg^{2+} and 1 mM ethylene glycol-bis- (β-aminoethyl ether) N,N,N′N′-tetraacetic acid (EGTA). For intracellular Ca^{2+} chelation, EGTA was included in the recording micropipette at a concentration of 200 mM. All drugs were purchased from Sigma. Extracellular concentric bipolar electrodes (FHC) were used to induce synaptic responses by local stimulation. Electrophysiological data were analysed using Clampfit 8.2 (Axon Inst.), Origin 6.0 (Microcal) and Matlab (Mathworks) software packages. Spectral (Fourier) analysis was conducted using Origin (spectral resolution 0.305 Hz) and the peristimulus histogram was plotted with Matlab software.

1. Goldman-Rakic, P. S. Cellular basis of working memory. *Neuron* **14,** 477–485 (1995).
2. Fuster, J. M. Network memory. *Trends Neurosci.* **20,** 451–459 (1997).
3. Insausti, R., Herrero, M. T. & Witter, M. P. Entorhinal cortex of the rat: cytoarchitectonic subdivisions and the origin and distribution of cortical efferents. *Hippocampus* **7,** 146–183 (1997).
4. Scoville, W. B. & Milner, B. Loss of recent memory after bilateral hippocampal lesions. *J. Neurol. Neurosurg. Psychiat.* **20,** 11–21 (1957).
5. Squire, L. R. & Zola-Morgan, S. The medial temporal lobe memory system. *Science* **253,** 1380–1386 (1991).
6. Young, B., Otto, T., Fox, G. D. & Eichenbaum, H. Memory representation within the parahippocampal region. *J. Neurosci.* **17,** 5183–5195 (1997).
7. Suzuki, W. A., Miller, E. K. & Desimone, R. Object and place memory in the macaque entorhinal cortex. *J. Neurophysiol.* **78,** 1062–1081 (1997).
8. Bunsey, M. & Eichenbaum, H. Critical role of the parahippocampal region for paired-associate learning in rats. *Behav. Neurosci.* **107,** 740–747 (1993).
9. Higuchi, S. & Miyashita, Y. Formation of mnemonic neuronal responses to visual paired associates in inferotemporal cortex is impaired by perirhinal and entorhinal lesions. *Proc. Natl Acad. Sci. USA* **93,** 739–743 (1996).
10. Stern, C. E., Sherman, S. J., Kirchhoff, B. A. & Hasselmo, M. E. Medial temporal and prefrontal contributions to working memory tasks with novel and familiar stimuli. *Hippocampus* **11,** 337–346 (2001).
11. Room, P. & Groenewegen, H. J. Connections of the parahippocampal cortex. I. Cortical afferents. *J. Comp. Neurol.* **251,** 415–450 (1986).
12. Rempel-Clower, N. L. & Barbas, H. The laminar pattern of connections between prefrontal and anterior temporal cortices in the Rhesus monkey is related to cortical structure and function. *Cereb. Cortex* **10,** 851–865 (2000).
13. Naber, P. A., Lopes da Silva, F. H. & Witter, M. P. Reciprocal connections between the entorhinal cortex and hippocampal fields CA1 and the subiculum are in register with the projections from CA1 to the subiculum. *Hippocampus* **11,** 99–104 (2001).
14. Alonso, J. R. & Amaral, D. G. Cholinergic innervation of the primate hippocampal formation. I. Distribution of choline acetyltransferase immunoreactivity in the *Macaca fascicularis* and *Macaca mulatta* monkeys. *J. Comp. Neurol.* **355,** 135–170 (1995).
15. Hasselmo, M. E. Neuromodulation: acetylcholine and memory consolidation. *Trends Cogn. Sci* **3,** 351–359 (1999).
16. Krnjevic, K. Central cholinergic mechanisms and function. *Prog. Brain Res.* **1993,** 285–292 (1993).
17. Hamam, B. N., Kennedy, T. E., Alonso, A. & Amaral, D. G. Morphological and electrophysiological characteristics of layer V neurons of the rat medial entorhinal cortex. *J. Comp. Neurol.* **418,** 457–472 (2000).
18. Andrade, R. Cell excitation enhances muscarinic cholinergic responses in rat association cortex. *Brain Res.* **548,** 81–93 (1991).
19. Fraser, D. D. & MacVicar, B. A. Cholinergic-dependent plateau potential in hippocampal CA1 pyramidal neurons. *J. Neurosci.* **16,** 4113–4128 (1996).
20. Haj-Dahmane, S. & Andrade, R. Ionic mechanism of the slow afterdepolarization induced by muscarinic receptor activation in rat prefrontal cortex. *J. Neurophysiol.* **80,** 1197–1210 (1998).
21. Klink, R. & Alonso, A. Muscarinic modulation of the oscillatory and repetitive firing properties of entorhinal cortex layer II neurons. *J. Neurophysiol.* **77,** 1813–1828 (1997).
22. Fransén, E., Alonso, A. A. & Hasselmo, M. E. Simulations of the role of the muscarinic-activated calcium-sensitive nonspecific cation current INCM in entorhinal neuronal activity during delayed matching tasks. *J. Neurosci.* **22,** 1081–1097 (2002).
23. Boeijinga, P. H. & Lopes da Silva, F. H. Modulations of EEG activity in the entorhinal cortex and forebrain olfactory areas during odour sampling. *Brain Res.* **478,** 257–268 (1989).
24. Wang, X.-J. Synaptic reverberation underlying mnemonic persistent activity. *Trends Neurosci.* **24,** 427–488 (2001).
25. Partridge, L. D. & Valenzuela, C. F. Block of hippocampal CAN channels by flufenamate. *Brain Res.* **867,** 143–148 (2000).
26. Lisman, J. E., Fellous, J. M. & Wang, X. J. A role for NMDA-receptor channels in working memory. *Nature Neurosci.* **1,** 273–275 (1998).
27. Seung, H. S., Lee, D. D., Reis, B. Y. & Tank, D. W. Stability of the memory of eye position in a recurrent network of conductance-based model neurons. *Neuron* **26,** 259–271 (2000).
28. Insausti, R., Amaral, D. G. & Cowan, W. M. The entorhinal cortex of the monkey: II. Cortical afferents. *J. Comp. Neurol.* **264,** 356–395 (1987).
29. Marder, E., Abbott, L. F., Turrigiano, G. G., Liu, Z. & Golowasch, J. Memory from the dynamics of intrinsic membrane currents. *Proc. Natl Acad. Sci. USA* **93,** 13481–13486 (1996).
30. Dickson, C. T. & Alonso, A. Muscarinic induction of synchronous population activity in the entorhinal cortex. *J. Neurosci.* **17,** 6729–6744 (1997).

The F-box protein Slimb controls the levels of clock proteins Period and Timeless

Brigitte Grima*, **Annie Lamouroux***, **Elisabeth Chélot***, **Christian Papin***, **Bernadette Limbourg-Bouchon**† & **François Rouyer***

* *Institut de Neurobiologie Alfred Fessard (NGI, CNRS UPR 2216) and* † *Centre de Génétique Moléculaire (CNRS UPR 2167), Centre National de la Recherche Scientifique, av. de la terrasse, 91198 Gif-sur-Yvette, France*

The *Drosophila* circadian clock is driven by daily fluctuations of the proteins Period and Timeless, which associate in a complex and negatively regulate the transcription of their own genes[1,2]. Protein phosphorylation has a central role in this feedback loop, by controlling Per stability in both cytoplasmic and nuclear compartments[3–6] as well as Per/Tim nuclear transfer[7,8]. However, the pathways regulating degradation of phosphorylated Per and Tim are unknown. Here we show that the product of the *slimb* (*slmb*) gene[9]—a member of the F-box/WD40 protein family of the ubiquitin ligase SCF complex that targets phosphorylated proteins for degradation[10–13]—is an essential component of the *Drosophila* circadian clock. *slmb* mutants are behaviourally